

Evidence of Multiple r-Process Sites in the Early Galaxy: New Observations of CS 22892-052¹

Christopher Sneden², John J. Cowan³, Inese I. Ivans², George M. Fuller⁴,
Scott Burles⁵, Timothy C. Beers⁶, James E. Lawler⁷

To appear in *The Astrophysical Journal Letters*

Received _____; accepted _____

¹Based on observations obtained with the Keck I Telescope of the W. M. Keck Observatory, which is operated by the California Association for Research In Astronomy (CARA, Inc) on behalf of the University of California and the California Institute of Technology.

²Department of Astronomy and McDonald Observatory, University of Texas, Austin, TX 78712; chris@verdi.as.utexas.edu, iivans@astro.as.utexas.edu

³Department of Physics and Astronomy, University of Oklahoma, Norman, OK 73019; cowan@phyast.nhn.ou.edu

⁴Department of Physics, University of California at San Diego, La Jolla, CA 92093-0319; gfuller@ucsd.edu

⁵Department of Astronomy and Astrophysics, University of Chicago, Chicago, IL 60637; burles@uchicago.edu

⁶Department of Physics and Astronomy, Michigan State University, East Lansing, MI 48824; beers@pa.msu.edu

⁷Department of Physics, University of Wisconsin, Madison, WI 53706; jelawler@facstaff.wisc.edu

ABSTRACT

First results are reported of a new abundance study of neutron-capture elements in the ultra-metal-poor (UMP; $[Fe/H] = -3.1$) halo field giant star CS 22892-052. Using new high resolution, high signal-to-noise spectra, abundances of more than 30 neutron-capture elements ($Z > 30$) have been determined. Six elements in the $40 < Z < 56$ domain (Nb, Ru, Rh, Pd, Ag and Cd) have been detected for the first time in a UMP star. Abundances are also derived for three of the heaviest stable elements (Os, Ir, and Pb). A second transition of thorium, Th II $\lambda 4086 \text{ \AA}$, confirms the abundance deduced from the standard Th II $\lambda 4019 \text{ \AA}$ line, and an upper limit to the abundance of uranium is established from the absence of the U II $\lambda 3859 \text{ \AA}$ line. As found in previous studies, the abundances of the heavier ($Z \geq 56$) stable neutron-capture elements in CS 22892-052 match well the scaled solar system r-process abundance distribution. From the observed Th abundance, an average age of $\simeq 16 \pm 4$ Gyr is derived for CS 22892-052, consistent with the lower age limit of $\simeq 11$ Gyr derived from the upper limit on the U abundance. The concordance of scaled solar r-process and CS 22892-052 abundances breaks down for the lighter neutron-capture elements, supporting previous suggestions that different r-process production sites are responsible for lighter and heavier neutron-capture elements.

Subject headings: stars: abundances — stars: Population II — Galaxy: halo — Galaxy: abundances — nuclear reactions, nucleosynthesis, abundances

1. Introduction

Ultra-metal-poor (UMP) stars serve a critical role for understanding the initial epochs of our Galaxy; the observed abundances in these very old stars provide clues to the nucleosynthetic processes in the earliest Galactic stellar generations. The UMP halo giant CS 22892-052 ($[\text{Fe}/\text{H}] = -3.1^8$) merits special attention in nucleosynthesis studies. This star has extremely large overabundances of neutron-capture (n-capture) elements relative to iron, and the abundances of those elements with $Z \geq 56$ apparently are consistent only with a scaled solar system r[apid]-process abundance distribution (Sneden *et al.* 1996; Cowan *et al.* 1999; Norris, Ryan, & Beers 1997; Pfeiffer, Kratz & Thielemann 1997). In addition, this is the first star for which thorium and an extensive number of n-capture elements have been detected, allowing an estimation of its radioactive age (Sneden *et al.* 1996; Cowan *et al.* 1997, 1999; Pfeiffer *et al.* 1997). Thus far, two n-capture element domains in CS 22892-052 and other UMP stars have been largely unexplored: the region $40 < Z < 56$ (between Zr and Ba); and the region $75 < Z < 83$ (the 3rd n-capture peak peak, Os→Pb). Using extensive new high resolution spectroscopic data, we have derived a new model-atmosphere for CS 22892-052, and derived abundances for a set of n-capture elements never before seen in this (or any other UMP) star. These new abundances and their implications for early Galactic nucleosynthesis of n-capture elements are discussed in this *Letter*.

⁸ $[\text{A}/\text{B}] \equiv \log_{10}(\text{N}_\text{A}/\text{N}_\text{B})_\text{star} - \log_{10}(\text{N}_\text{A}/\text{N}_\text{B})_\odot$, and $\log \varepsilon(\text{A}) \equiv \log_{10}(\text{N}_\text{A}/\text{N}_\text{H}) + 12.0$, for elements A and B. UMP stars are considered to be those with $[\text{Fe}/\text{H}] < -2.5$.

2. Observations, Reductions, and Abundance Analysis

Two new high resolution, high S/N spectra of CS 22892-052 were obtained. The Keck I HIRES (Vogt *et al.* 1994) was used for one night in August, 1998 to obtain a spectrum (the sum of multiple individual integrations) in the near-UV region, $3200 \lesssim \lambda \lesssim 4250 \text{ \AA}$. The resolving power was $R \equiv \lambda/\Delta\lambda \simeq 45,000$, and the S/N varied smoothly from ~ 30 near $\lambda 3200 \text{ \AA}$ to $\gtrsim 200$ near $\lambda 4250 \text{ \AA}$. We also used the McDonald 2.7m Smith telescope and 2d-coudé echelle spectrograph (Tull *et al.* 1995) for three nights in October, 1998 to obtain a high resolution ($R \simeq 60,000$) spectrum, also the sum of multiple exposures, at longer wavelengths ($4400 \lesssim \lambda \lesssim 8000 \text{ \AA}$). Again, the S/N varied with wavelength, from ~ 50 near $\lambda 4500 \text{ \AA}$ to $\gtrsim 150$ near $\lambda 7000 \text{ \AA}$. Accompanying both HIRES and 2d-coudé observations of CS 22892-052 were standard auxiliary integrations on tungsten filament and Th-Ar hollow cathode lamps. For the 2d-coudé data, observations of hot, rapidly rotating (essentially featureless) stars of similar airmass to CS 22892-052 were obtained to facilitate removal of telluric spectral features in the longer wavelength spectral regions. Standard echelle reduction techniques were used to produce the final spectra.

We determined new model atmosphere parameters for CS 22892-052 from an analysis of equivalent widths (mostly from uncrowded longer wavelength spectral regions) of nearly 200 transitions of lighter ($Z \leq 30$) elements. This analysis applied the usual conditions that demand agreement between abundances from low- and high-excitation lines and from weak and strong lines of a given species, and agreement between neutral and ionized species abundances. We interpolated model atmospheres from the Kurucz (1999) grid, and employed the current version of Sneden's (1973) line analysis code. The derived model has $T_{\text{eff}} = 4710 \text{ K}$, $\log g = 1.50$, $v_t = 2.1 \text{ km s}^{-1}$, and model metallicity $[\text{M}/\text{H}] = -3.2$. These values are in good agreement with the parameters (4760 K, 1.30, 2.3 km s^{-1} , -3.1) determined previously by McWilliam *et al.* (1995) from lower resolution, lower S/N spectra.

Our new abundances for the $Z \leq 30$ elements also agree well with those of McWilliam *et al.*, but with greatly reduced line-to-line scatter.

With the new model atmosphere, abundances for n-capture elements were determined from equivalent width and synthetic spectrum analyses. The analysis techniques are described in detail by Sneden *et al.* (1996). Table 1 gives the new abundances and their single-line standard deviation values, as well as abundances that were determined by Sneden *et al.*. We first analyzed some n-capture elements (Y, Zr, Nd, Sm, Eu, Gd, Dy, Er, Tm, and Yb) previously treated by Sneden *et al.*. These elements have large numbers of transitions in the near-UV ($\lambda < 4000 \text{ \AA}$). The new analyses used the enlarged spectral coverage of our new CS 22892-052 data and the most recent oscillator strength information in greatly expanding the line lists for these elements. The reliability of the abundances increased, as indicated by lower σ values for most of the re-analyzed elements. The new abundances are in good accord with those of Sneden *et al.*. Moreover, there are no discernible abundance trends for individual n-capture element species with wavelength, suggesting that the model atmosphere and line analysis techniques consistently reproduce the observed CS 22892-052 spectrum from the red to the near-UV spectral regions.

We then searched the spectra for transitions of n-capture elements not previously detected in UMP (or in fact, in most) stars. This yielded detections of six light n-capture elements (Nb, Ru, Rh, Pd, Ag, and Cd). Additionally, some elements of the 3rd n-capture peak (Os, Ir, and Pb) were identified; of this group only Os had previously been tentatively detected by Sneden *et al.* (1996). We derived abundances for these elements via synthetic spectrum computations, since their transitions lie mainly in the crowded near-UV spectral region. For illustration, in Figure 1 we present the observed and synthetic spectra of lines for three of the elements. These transitions and other new ones were easily identified even in the lowest wavelength spectral regions. In Table 1 we list the abundances of these newly

identified elements. Note that Nb, Ru, and Cd have only one transition so far identified on our spectra. The (relatively large) σ values for these elements represent conservative estimates from assessment of transition probability information, continuum placement, identification of blending spectral features, and synthetic spectrum fits.

Finally, we considered the radioactive chronometer elements thorium and uranium. We detected a new Th II line at $\lambda 4086.52 \text{ \AA}$, and analyzed that line in conjunction with the usually-employed $\lambda 4019.12 \text{ \AA}$ line. The abundances from these two transitions are in excellent agreement, and are very similar to the Th abundance determined by Sneden *et al.* (1996). We did not find any features of U II, but derived an upper limit to the U abundance from an estimate of the maximum strength of the un-detected $\lambda 3859.57 \text{ \AA}$ feature.

3. Discussion and Conclusions

In the top panel of Figure 2 we plot the CS 22892-052 n-capture abundances from this study, and those of Sneden *et al.* (1996) for elements not analyzed by us. A scaled solar system r-process elemental abundance distribution is also shown. The solar distribution is obtained by a decomposition of the solar system elemental abundances (Anders & Grevesse 1989) into s[low]- and r-process contributions to individual isotopes, and is based upon the measured isotopic n-capture cross sections (Käppeler *et al.* 1989, Wissak *et al.* 1996). Summation of those contributions produces a solar system r-process *elemental* abundance curve; see Burris *et al.* (2000) for details of this procedure. The solar system curve has been shifted to match the mean abundance level of the heavier n-capture elements ($56 \leq Z \leq 72$) in CS 22892-052. The mean difference is $\langle \log \epsilon_{\text{CS 22892-052}} - \log \epsilon_{\text{s.s.}} \rangle = -1.41 \pm 0.02$ ($\sigma = 0.08$, 15 elements). The small scatter about the mean value confirms and extends all previous studies that have found consistency between CS 22892-052 heavy n-capture element abundances and the solar system r-process distribution. In the bottom panel

of Figure 2 this agreement is shown via a plot of the differences $\delta(\log \epsilon)$ between the CS 22892-052 abundances and the scaled solar curve.

Abundances of the 3rd n-capture peak elements Os, Ir, and Pb are also in good agreement with the scaled solar system r-process distribution. Abundances of 3rd peak elements in two other UMP stars (*e.g.*, Sneden *et al.* 1998) have anticipated this result, but these are the first reliable 3rd peak abundances in CS 22892-052. Thus the solar r-process pattern extends throughout the $56 \leq Z \leq 82$ element domain in this star.⁹ A nearly identical abundance distribution is observed in the UMP star HD 115444 (Westin *et al.* 2000). In addition, the [Ba/Eu] ratio in most UMP stars is in accord with the solar r-process value (*e.g.*, McWilliam 1998, Burris *et al.* 2000). The agreement of all of these abundance patterns with the solar system r-process distribution suggests a uniform site, and/or uniform conditions for synthesis of the heavier n-capture elements.

The thorium abundance of CS 22892-052 lies below the solar r-process curve in Figure 2, indicating that radioactive decay of this element has taken place over the time since it was created by the progenitor of this star. We computed a Th-based radioactive age for CS 22892-052 with various input assumptions (such as using both theoretical r-process predictions and the observed solar system abundances). The calculations are sensitive to small parameter changes and give a range of results with a average of $\simeq 16$ Gyr. The error bars on the derived age, including both observational and theoretical uncertainties, are $\simeq 4$ Gyr. An age estimate for CS 22892-052 from the upper limit on the uranium abundance can be done by comparing this limit with predictions (Cowan *et al.* 1999) for the long-lived uranium ^{238}U isotope (*i.e.*, assuming that we are not observing any of the relatively quickly decaying ^{235}U isotope). This yields a lower age limit of $\simeq 11$ Gyr for CS 22892-052. While

⁹ The Pb abundance is based on extremely weak transitions, and remains poorly determined.

this limit is even more uncertain than values based upon the detection of Th, it does provide a lower bound on the age of this star which, within the error uncertainty, is consistent with the age determination using the Th chronometer.

In contrast to the heavy stable elements, our observations clearly demonstrate that the agreement between CS 22892-052 and solar system r-process abundances fails for the lighter ($Z < 56$) n-capture elements (see Figure 2). For these nine elements, $\langle \log \epsilon_{\text{CS 22892-052}} - \log \epsilon_{\text{s.s.}} \rangle = -1.72 \pm 0.07$ ($\sigma = 0.20$). Abundances of six of the lighter n-capture elements lie well below the solar system r-process curve that reproduces the heavier elements. The abundances of the odd-Z light n-capture elements are substantially less than those of the even-Z elements, a pattern typically seen in s-process nucleosynthesis. However, the scaled solar system s-process abundance distribution is a poor match to the CS 22892-052 lighter n-capture abundances. Numerical experiments, analogous to those conducted by Cowan *et al.* (1995), suggest that a mix consisting of solar r-process abundances plus 10% of the solar s-process abundances can roughly fit the CS 22892-052 data. But the Y and Ag abundances of CS 22892-052 are 0.3-0.5 dex lower than this hybrid solar system distribution. In addition, the overall abundance level of these elements is still about 0.2 dex below the level of the heavier elements, when compared together to the solar distribution (Figure 2). There does not appear to be a simple way to mix solar n-capture abundances to match those of CS 22892-052.

The existence of two distinct r-process signatures in solar system meteoritic material, one for n-capture nuclei lighter than mass number 140 and one for heavier nuclei, has been previously suggested by Wasserburg, Busso, & Gallino (1996), Qian, Vogel, & Wasserburg (1998). The clear differences between the abundances of the heavier and the lighter r-process elemental abundances in CS 22892-052 are consistent with that suggestion. Thus lighter and heavier nuclei possibly could be produced on different Galactic timescales and

come from supernovae of different mass ranges (Qian & Wasserburg 2000). Alternatively, neutron-star binaries also could be a source for one of the mass ranges of r-process nuclei (Rosswog *et al.* 1999).

The total n-capture CS 22892-052 abundance pattern is also consistent with a neutrino-heated supernova ejecta r-process in a single supernova event, albeit with two different epochs in the explosion/ejection process (*cf.*, Woosley *et al.* 1994, and references therein). In neutrino-heated ejecta nucleosynthesis models the abundance yields are extremely sensitive to the electron fraction in the shock re-heating epoch when the lighter r-process species are synthesized (Hoffman *et al.* 1996). The electron fraction and the resulting lighter r-process abundances in this early epoch are expected to be different for each supernova event. By contrast, the later neutrino-driven wind epoch, where the heavier r-process nuclides originate in these models, should have similar conditions, therefore producing the same abundance pattern, in all supernovae.

An additional clue about early Galactic n-capture nucleosynthesis lies in the now well-documented very large star-to-star scatter in the bulk [n-capture/Fe] ratios of UMP stars (*e.g.*, McWilliam *et al.* 1995, Burris *et al.* 2000). In CS 22892-052 for example, $[\text{Eu}/\text{Fe}] \sim +1.6$ (Sneden *et al.* 1996), while other UMP stars have $[\text{Eu}/\text{Fe}] < 0$. The large scatter in overall n-capture element content is an indication of the chemical inhomogeneity of the Galactic halo; the Galaxy was not well-mixed at very early epochs. Possible explanations for the early scatter in the [n-capture/Fe] ratio involve separating the iron and r-process production into different types of supernovae with an initial iron production from very massive stars (Wasserburg & Qian 2000). Detailed abundance analyses of many very low metallicity stars, and more extensive theoretical r-process calculations will be needed to understand better the differences between the production of iron and the entire range of r-process elements in the earliest Galactic stellar populations.

We thank Andy McWilliam, George Preston, Jim Truran, and Craig Wheeler for helpful discussions, and the referee, Jerry Wasserburg, for helping us to improve the paper. We are grateful to the staff of the Keck Observatory for their expert assistance with the observations. This research was funded in part by NSF grants AST-9618364 to CS, AST-9618332 to JJC, AST-9529454 to TCB, and PHY-9800980 to GMF.

REFERENCES

Anders, E., & Grevesse, N. 1989, *Geochim. Cosmochim. Acta*, 53, 197

Burris, D. L., Pilachowski, C. A., Armandroff, T., Sneden, C., Roe, H., & Cowan, J. J. 2000, *ApJ*, submitted

Cowan, J. J., Burris, D. L., Sneden, C., Preston, G. W., & McWilliam, A. 1995, *ApJ*, 439, L51

Cowan, J. J., McWilliam, A., Sneden, C., & Burris, D. L. 1997, *ApJ*, 480, 246

Cowan, J. J., Pfeiffer, B., Kratz, K.-L., Thielemann, F.-K., Sneden, C., Burles, S., Tytler, D., & Beers, T. C. 1999, *ApJ*, 521, 194

Hoffman, R. D., Woosley, S. E., Fuller, G. M., & Meyer, B. S. 1996 *ApJ*, 460, 478.

Käppeler, F., Beer, H., & Wissak, K. 1989, *Rep. Prog. Phys.*, 52, 945

Kurucz, R. L. 1999, <http://cfaku5.harvard.edu>

McWilliam, A. 1998, *AJ*, 115, 1640

McWilliam, A., Preston, G. W., Sneden, C., & Shectman, S. 1995, *AJ*, 109, 2757.

Norris, J. E., Ryan, S. G., & Beers, T. C. 1997, *ApJ*, 488, 350

Pfeiffer, B., Kratz, K.-L., & Thielemann, F.-K. 1997, *Z. Phys. A*, 357, 235

Qian, Y.-Z., Vogel, P., & Wasserburg, G. J. 1998, *ApJ*, 506, 868

Qian, Y.-Z., & Wasserburg, G. J. 2000, *ApJ*, 529, L21

Rosswog, S., Liebendorfer, M., Thielemann, F.-K., Davies, M. B., Benz, W., & Piran, T., 1999, *A&A*, 341, 499

Sneden, C. 1973, ApJ, 184, 839

Sneden, C., Cowan, J. J., Burris, D. L., & Truran, J. W. 1998, ApJ, 496, 235

Sneden, C., McWilliam, A., Preston, G. W., Cowan, J. J., Burris, D. L., & Armosky, B. J. 1996, ApJ, 467, 819

Tull, R. G., MacQueen, P. J., Sneden, C., & Lambert, D. L. 1995, PASP, 107, 251

Vogt, S. S., *et al.* 1994, in Proc. SPIE Conf. 2198, Instrumentation in Astronomy VII, ed. D. L. Crawford & E. R. Craine (Bellingham, WA: SPIE), 362

Wasserburg, G. J., Busso, M., & Gallino, R. 1996, ApJ, 466, 109

Wasserburg, G. J., & Qian, Y.-Z. 2000, ApJ, 529, L21

Westin, J., Sneden, C., Gustafsson, B., & Cowan, J. J. 2000, ApJ, in press

Wissak, K., Voss, F., & Käppeler, F. 1996, in Proceedings of the 8th Workshop on Nuclear Astrophysics, ed. W. Hillebrandt, & E. Müller (Munich: MPI), 16

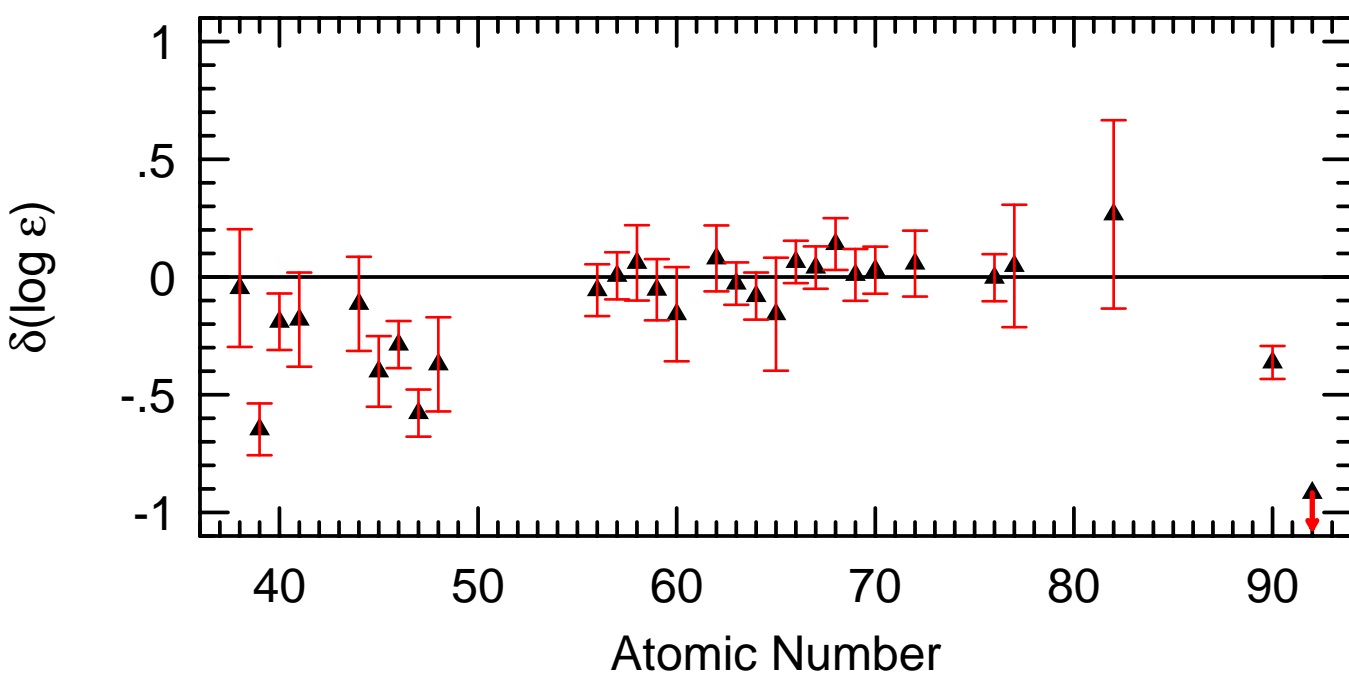
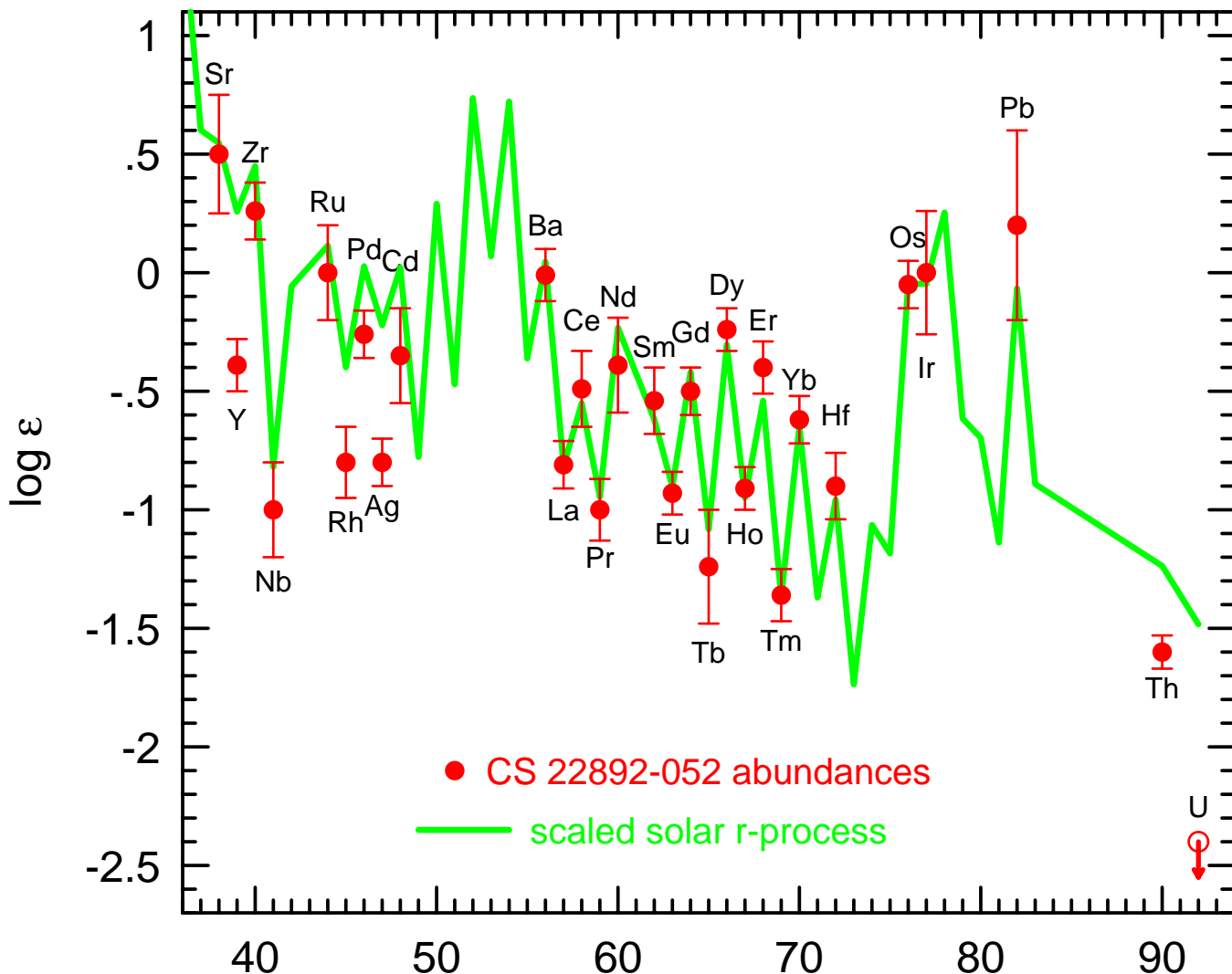
Woosley, S. E., Wilson, J. R., Mathews, G. J., Hoffman, R. D., & Meyer, B. S. 1994, ApJ, 433, 229

Figure Captions

Fig. 1.— Observed spectra (filled circles) and synthetic spectra (solid lines) are shown for three representative transitions of newly detected n-capture elements in CS 22892-052. The abundances assumed in generating the synthetic spectra of Pd I $\lambda 3404$ Å (top panel), Ag I $\lambda 3281$ Å (middle panel), and Ir I $\lambda 3514$ Å (lower panel) are noted in the respective panels.

Fig. 2.— In the top panel, n-capture abundances in CS 22892-052 are plotted as filled circles with error bars, along with a scaled solar system *r*-process abundance curve that is plotted as a solid line. See the text for explanation of how the match between stellar and solar system distributions was accomplished. Note also the abundance of Th, sitting well below the scaled solar system curve, and the (very low) upper limit for U indicated by an open symbol with an arrow. In the bottom panel, a differential comparison is presented between individual elements and the scaled solar system *r*-process abundance distribution. The ordinate $\delta(\log \epsilon)$ represents the difference between the abundance of an individual element and the scaled solar curve. Again, an open symbol with an arrow denotes the U abundance upper limit.

Neutron-Capture Abundances in CS 22892-052



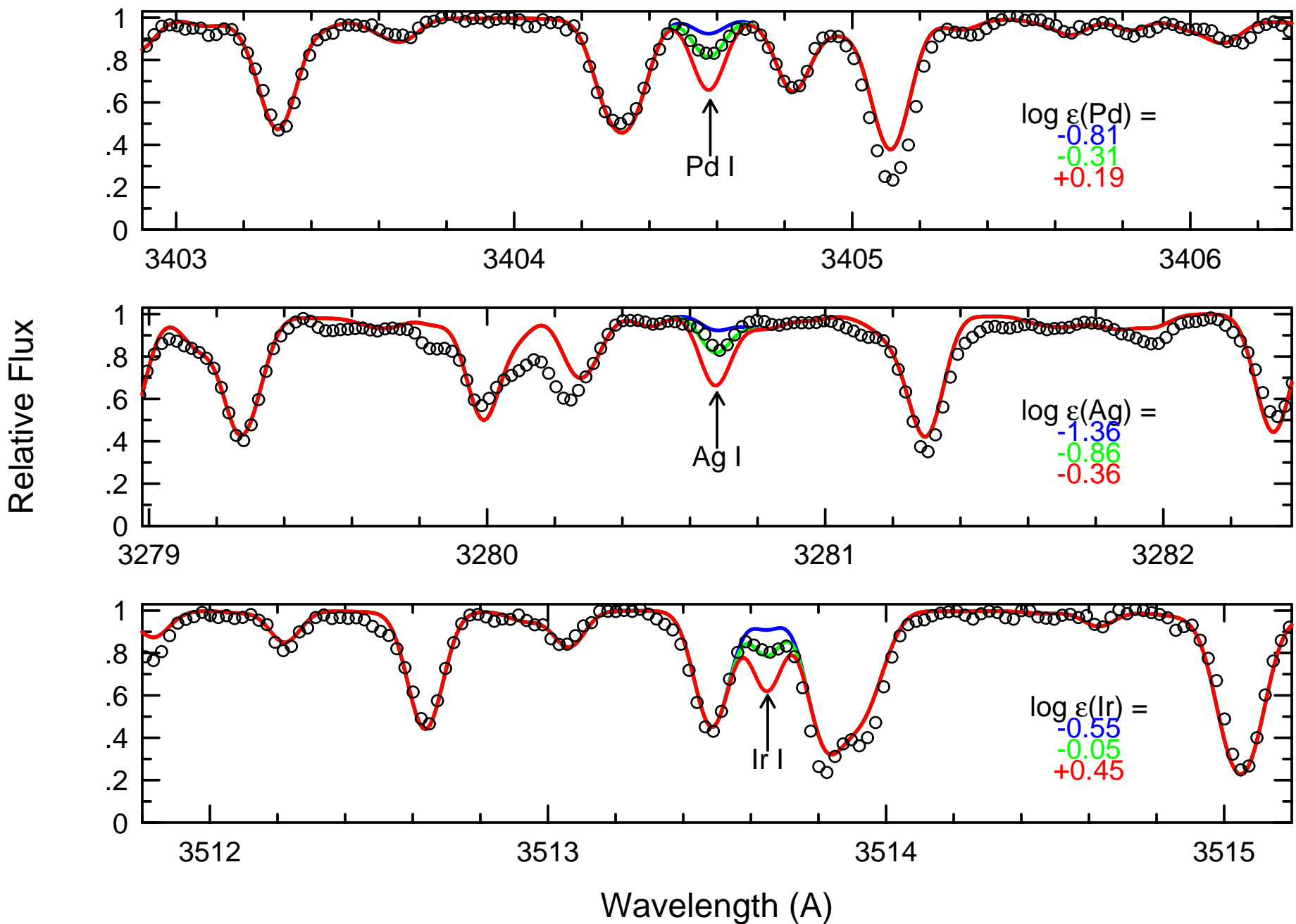


TABLE 1
ABUNDANCES FOR CS 22892-052

| Species | Z | $\log \epsilon$ | σ (CTIO) | # | $\log \epsilon$ | σ (2d-coudé,HIRES) | # |
|---------|----|-----------------|--------------------|----|-----------------|------------------------------|----|
| Sr I,II | 38 | +0.50 | 0.25 | 4 | ... | ... | 0 |
| Y II | 39 | -0.40 | 0.12 | 10 | -0.39 | 0.11 | 16 |
| Zr II | 40 | +0.30 | 0.14 | 5 | +0.26 | 0.12 | 28 |
| Nb II | 41 | ... | ... | 0 | -1.00 | 0.20 | 1 |
| Ru I | 44 | ... | ... | 0 | 0.00 | 0.20 | 1 |
| Rh I | 45 | ... | ... | 0 | -0.80 | 0.15 | 1 |
| Pd I | 46 | ... | ... | 0 | -0.26 | 0.10 | 3 |
| Ag I | 47 | ... | ... | 0 | -0.80 | 0.10 | 2 |
| Cd I | 48 | ... | ... | 0 | -0.35 | 0.20 | 1 |
| Ba II | 56 | -0.01 | 0.11 | 7 | ... | ... | 0 |
| La II | 57 | -0.81 | 0.10 | 7 | ... | ... | 0 |
| Ce II | 58 | -0.49 | 0.16 | 9 | ... | ... | 0 |
| Pr II | 59 | -1.00 | 0.13 | 6 | ... | ... | 0 |
| Nd II | 60 | -0.34 | 0.15 | 18 | -0.39 | 0.20 | 52 |
| Sm II | 62 | -0.63 | 0.16 | 9 | -0.54 | 0.14 | 17 |
| Eu II | 63 | -0.89 | 0.12 | 9 | -0.93 | 0.09 | 7 |
| Gd II | 64 | -0.50 | 0.16 | 7 | -0.50 | 0.10 | 20 |
| Tb II | 65 | -1.24 | 0.24 | 7 | ... | ... | 0 |
| Dy II | 66 | -0.38 | 0.15 | 7 | -0.24 | 0.09 | 27 |
| Ho II | 67 | -0.91 | 0.09 | 4 | ... | ... | 0 |
| Er II | 68 | -0.52 | 0.09 | 5 | -0.40 | 0.11 | 8 |
| Tm II | 69 | -1.36 | 0.11 | 4 | -1.37 | 0.05 | 5 |
| Yb II | 70 | -0.80 | 0.2 | 1 | -0.62 | 0.10 | 1 |
| Hf II | 72 | -0.90 | 0.14 | 2 | ... | ... | 0 |
| Os I | 76 | -0.10 | 0.38 | 3 | -0.05 | 0.10 | 3 |
| Ir I | 77 | ... | ... | 0 | 0.00 | 0.26 | 3 |
| Pb I | 82 | ... | ... | 0 | +0.20 | 0.4 | 2 |
| Th II | 90 | -1.55 | 0.08 | 1 | -1.60 | 0.07 | 2 |
| U II | 92 | ... | ... | 0 | <-2.4 | ... | 1 |